# Supporting Information

## Understanding Solid-State Solvation-Enhanced Thermally Activated Delayed Fluorescence Using a Descriptor-Tuned Screened Range-Separated Functional

*Chao Wang*, and Qisheng Zhang**

MOE Key Laboratory of Macromolecular Synthesis and Functionalization, Department of Polymer Science and Engineering, Zhejiang University, Hangzhou 310027, China

# Content

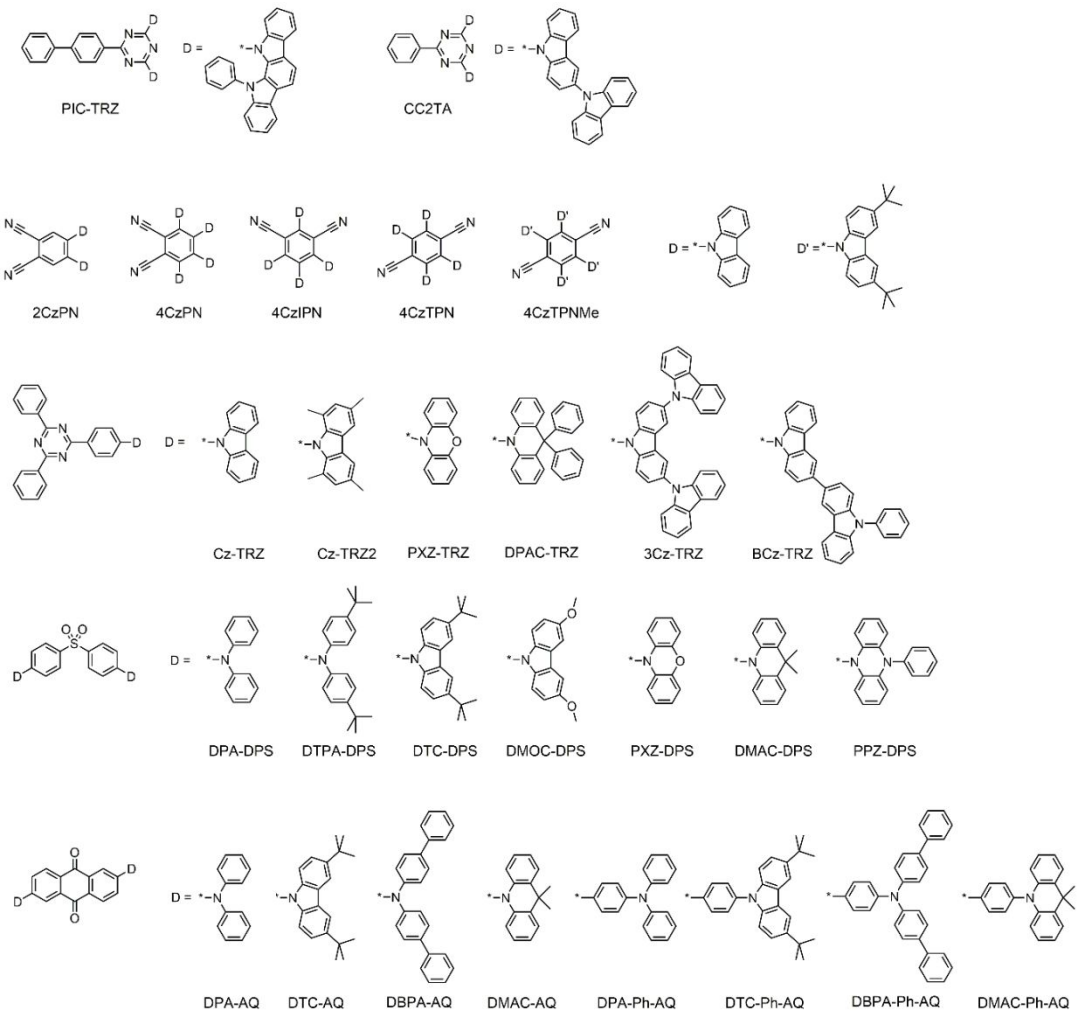


**Figure S1.** Chemical structures of TADF emitters calculated in this work.

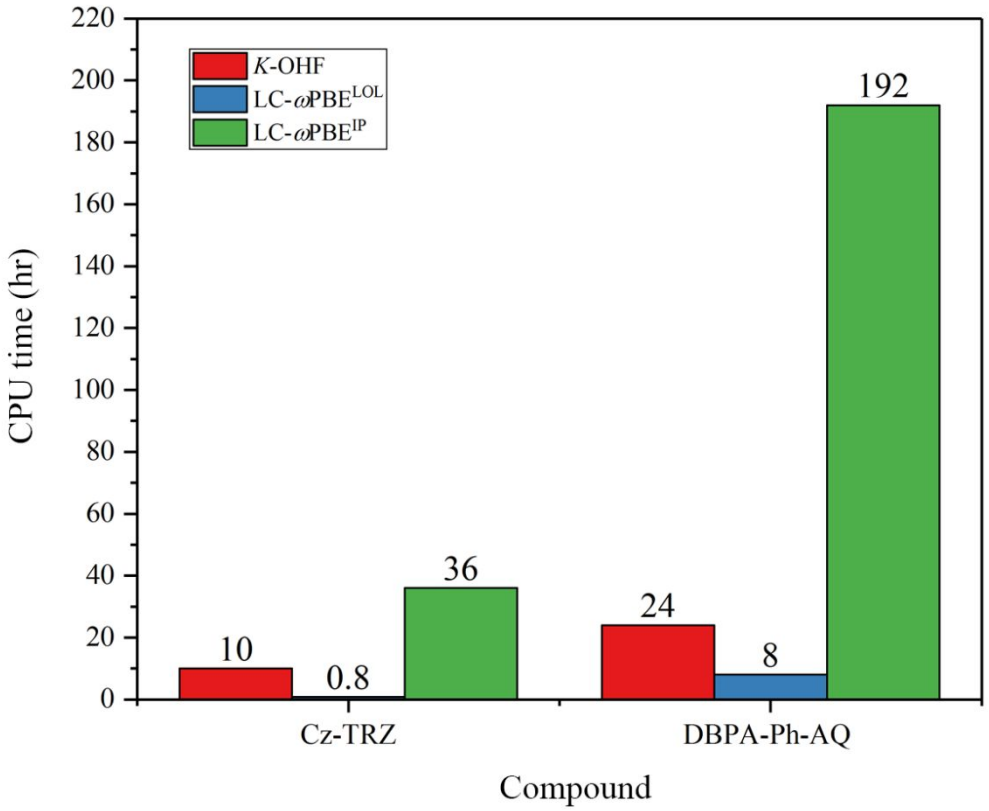


**Figure S2.** The job time of the tuning procedure of *K*-OHF, LOL- and IP-tuning scheme.

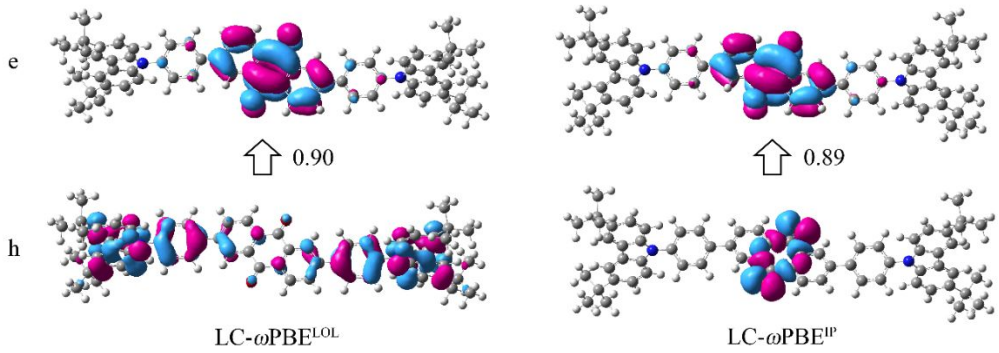


**Figure S3.** The distribution of the hole (h) and electron (e) NTOs (isovalue = 0.02) of the lowest absorption of DTC-Ph-AQ with the largest weight calculated at the TDA-LC-$\omega$PBE$^{LOL}$/6-311G(d) and TDA-LC-$\omega$PBE$^{IP}$/6-311G(d) levels in the PCM cyclohexane solvation.

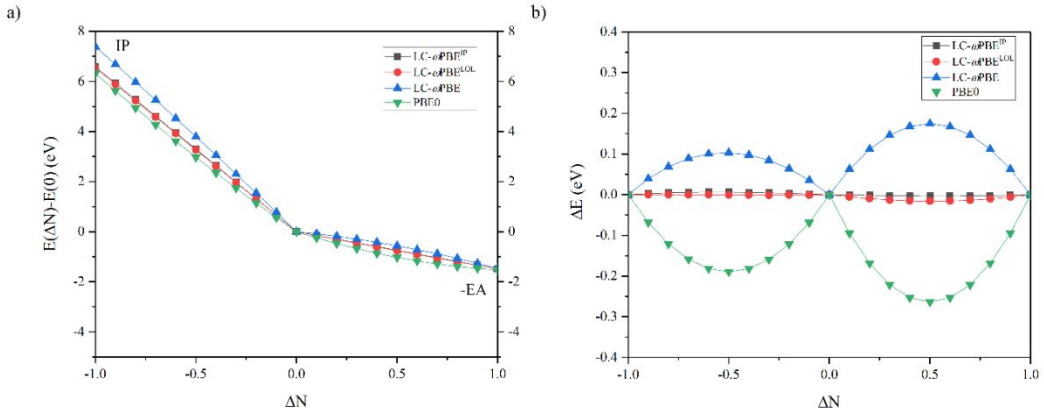


**Figure S4.** (a) The energy difference of the fractional charge number ($E$(ΔN)) to the neutral one ($E$(0)) for DBPA-AQ. (b) The deviation of the curves ($\Delta E$) to the straight lines in (a).

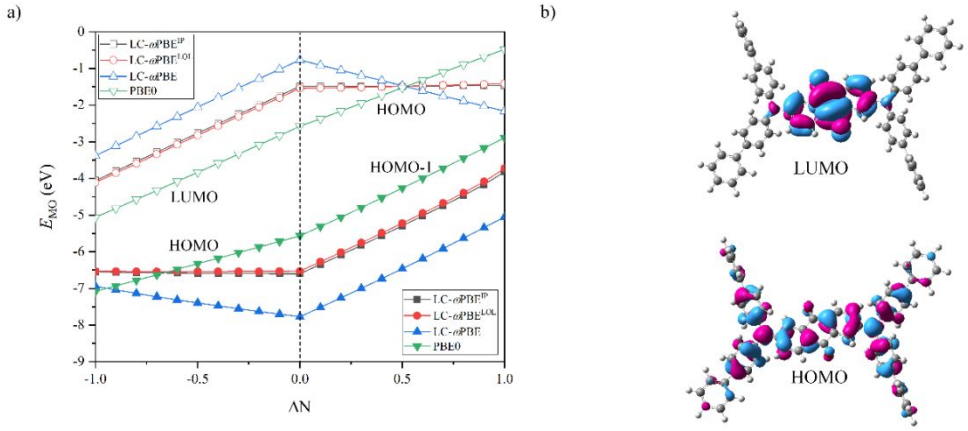


**Figure S5.** (a) The molecular orbital energy ($E_{MO}$) as a function of the fractional charge number (ΔN) in DBPA-AQ. (b) The distribution of the HOMO and LUMO in the neutral state (isovalue =0.02).

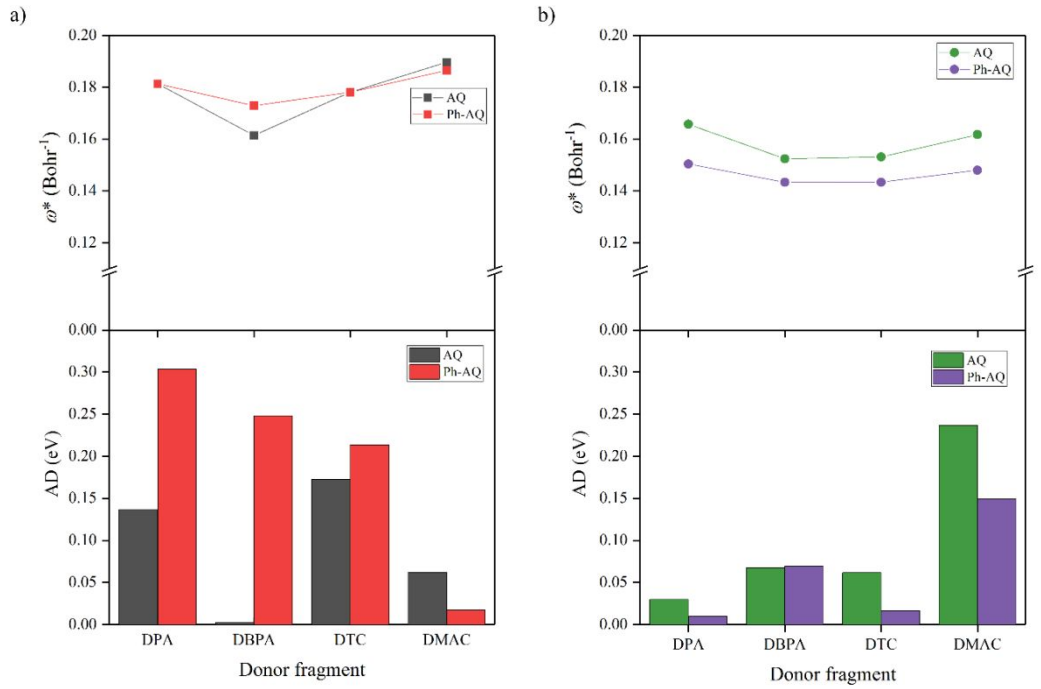


**Figure S6.** The $\omega$* and the absolute deviation of $E_{VA}(S_1)$ (AD) as functions of the donor fragment calculated at the (a) LC-$\omega$PBE$^{IP}$/6-311G(d); and (b) LC-$\omega$PBE$^{LOL}$/6-311G(d) levels of theory.

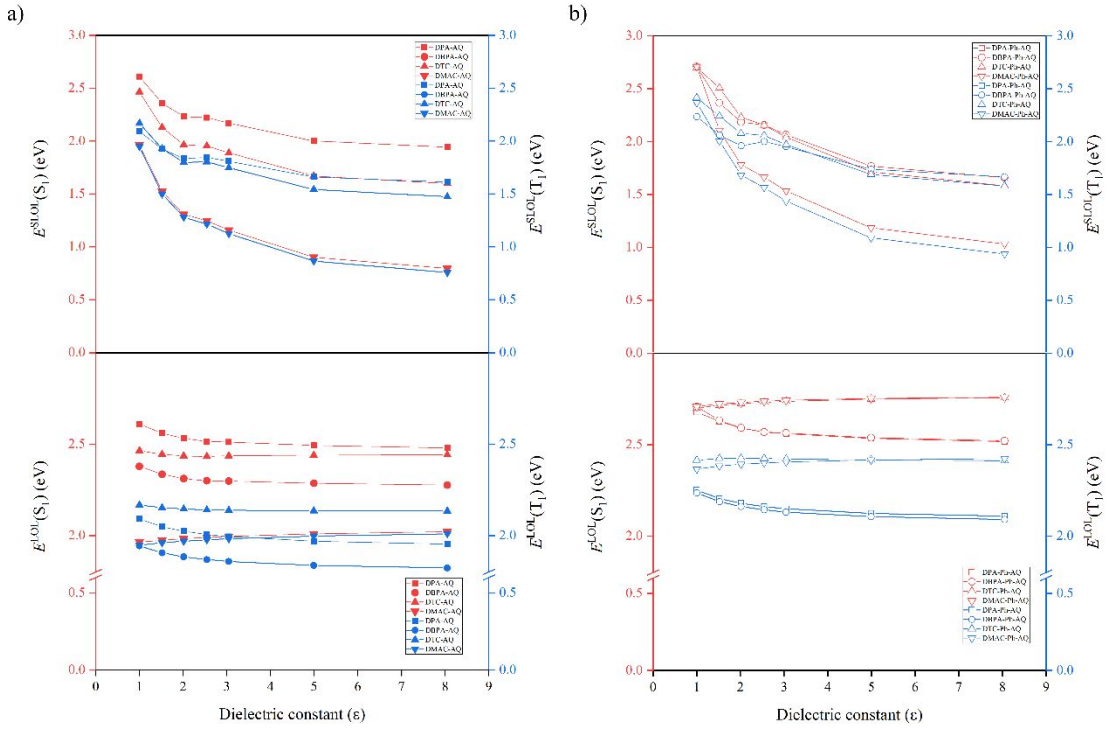


**Figure S7.** The $S_1$ and $T_1$ excited state energies ($E(S_1)$ and $E(T_1)$) as functions of the dielectric constant (ε) calculated at the TDA-LC-$\omega$PBE$^{LOL}$/6-311G(d) level in the PCM cyclohexane solvation and at the TDA-LC-$\omega$PBE$^{SLOL}$/6-311G(d) level in the (a) Donor-AQ series and (b) Donor-Ph-AQ series.

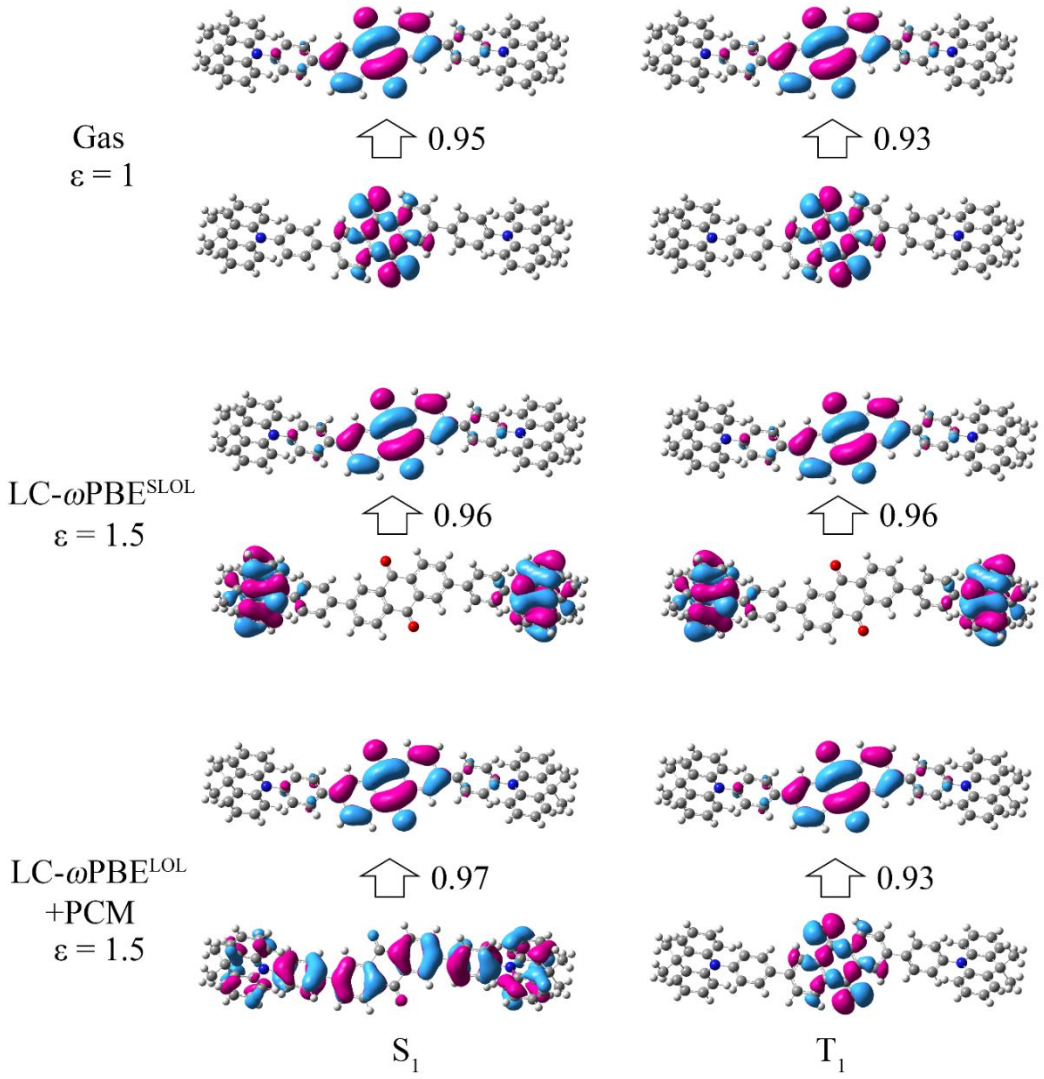


**Figure S8.** The hole and electron NTOs of $S_1$ and $T_1$ states with the corresponding weight based on the $S_0$ geometry of DMAC-Ph-AQ.

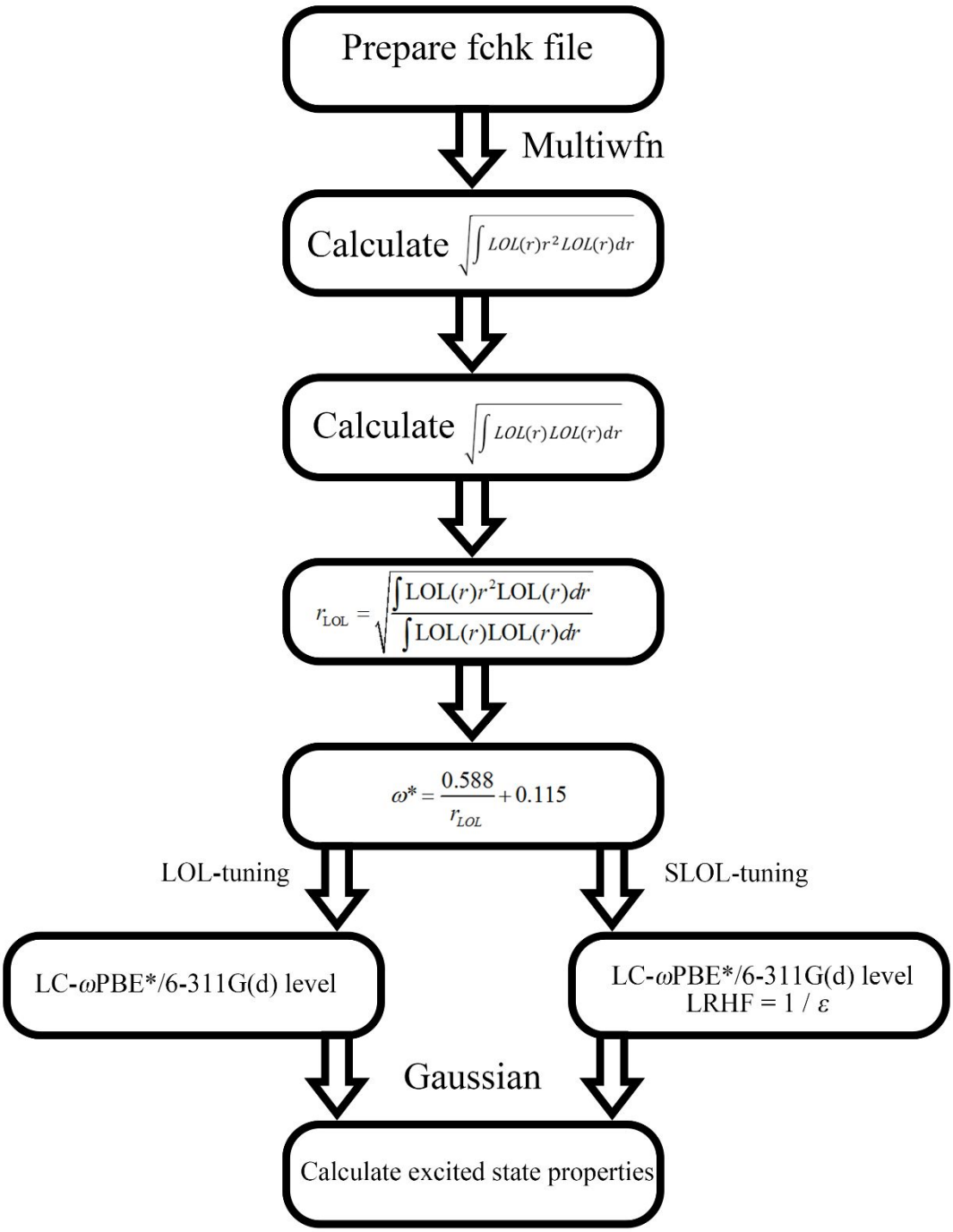


**Scheme S1.** The flowchart of LOL- and SLOL-tuning

**Table S1**. Training TADF molecules for establishing the $r_{LOL}$-$\omega$* relationship.

| Compound | $r_{LOL}$ (Bohr) | 1/ $r_{LOL}$(Bohr$^{-1}$) | $\omega$* (Bohr$^{-1}$) |
|---|---|---|---|
| PIC-TRZ | 10.695 | 0.094 | 0.160 |
| CC2TA | 13.302 | 0.075 | 0.157 |
| 2CzPN | 7.899 | 0.127 | 0.190 |

| | | | |
|---|---|---|---|
| 4CzIPN | 9.692 | 0.103 | 0.184 |
| Cz-TRZ2 | 11.252 | 0.089 | 0.167 |
| DTPA-DPS | 14.023 | 0.071 | 0.159 |
| DTC-DPS | 14.383 | 0.070 | 0.160 |
| DMOC-DPS | 12.657 | 0.079 | 0.160 |
| DPA-AQ | 11.597 | 0.086 | 0.164 |
| DPA-Ph-AQ | 16.614 | 0.060 | 0.150 |

**Table S2.** The LOL- and IP-tuned $\omega$* (Bohr $^{-1}$) and corresponding relaxation energy $\lambda$ (eV) at the optimized $S_0$, $S_1$ and $T_1$ geometry.

| Compound | $S_0$ | | $S_1$ | | | $T_1$ |
|---|---|---|---|---|---|---|
| | $\omega^{LOL}$ | $\omega^{IP}$ | $\omega^{LOL}$ | $\omega^{IP}$ | $\lambda^{LOL}$ | $\lambda^{LOL}$ |
| PIC-TRZ | 0.170 | 0.144 | 0.170 | 0.149 | 0.22 | 0.04 |
| CC2TA | 0.159 | 0.165 | 0.160 | 0.164 | 0.40 | 0.17 |
| PXZ-TRZ | 0.170 | 0.189 | 0.170 | 0.183 | 0.21 | 0.26 |
| DPAC-TRZ | 0.164 | 0.173 | 0.164 | 0.165 | 0.22 | 0.42 |
| Cz-TRZ | 0.169 | 0.183 | 0.169 | 0.174 | 0.13 | 0.28 |
| Cz-TRZ2 | 0.167 | 0.181 | 0.168 | 0.174 | 0.24 | 0.42 |
| 3Cz-TRZ | 0.157 | 0.175 | 0.157 | 0.160 | 0.17 | 0.20 |
| BCz-TRZ | 0.154 | 0.173 | 0.154 | 0.163 | 0.13 | 0.22 |
| 2CzPN | 0.189 | 0.182 | 0.192 | 0.191 | 0.48 | 0.36 |
| 4CzPN | 0.177 | 0.149 | 0.178 | 0.160 | 0.27 | 0.27 |
| 4CzIPN | 0.176 | 0.146 | 0.176 | 0.151 | 0.20 | 0.14 |
| 4CzTPN | 0.175 | 0.151 | 0.175 | 0.154 | 0.22 | 0.18 |
| 4CzTPNMe | 0.168 | 0.146 | 0.169 | 0.123 | 0.42 | 0.29 |
| DPA-DPS | 0.168 | 0.171 | 0.169 | 0.174 | 0.30 | 0.56 |
| DTPA-DPS | 0.157 | 0.156 | 0.158 | 0.162 | 0.39 | 0.70 |
| DTC-DPS | 0.156 | 0.165 | 0.156 | 0.173 | 0.29 | 0.09 |
| DMOC-DPS | 0.161 | 0.175 | 0.162 | 0.185 | 0.46 | 0.09 |
| PXZ-DPS | 0.168 | 0.183 | 0.166 | 0.189 | 0.15 | 0.30 |
| DMAC-DPS | 0.164 | 0.176 | 0.165 | 0.180 | 0.23 | 0.42 |
| PPZ-DPS | 0.159 | 0.173 | 0.158 | 0.174 | 0.20 | 0.20 |
| DPA-AQ | 0.166 | 0.181 | 0.166 | 0.181 | 0.18 | 0.15 |
| DBPA-AQ | 0.152 | 0.161 | 0.153 | 0.160 | 0.27 | 0.21 |
| DTC-AQ | 0.153 | 0.178 | 0.153 | 0.172 | 0.14 | 0.11 |
| DMAC-AQ | 0.162 | 0.190 | 0.162 | 0.183 | 0.17 | 0.15 |
| DPA-Ph-AQ | 0.150 | 0.181 | 0.151 | 0.178 | 0.27 | 0.31 |
| DBPA-Ph-AQ | 0.143 | 0.173 | 0.143 | 0.160 | 0.11 | 0.21 |
| DTC-Ph-AQ | 0.143 | 0.178 | 0.143 | 0.181 | 0.17 | 0.08 |
| DMAC-Ph-AQ | 0.148 | 0.187 | 0.148 | 0.187 | 0.19 | 0.13 |

[a]The relaxation energy of IP-tuning can be found in Ref. 1

**Table S3.** Comparison of the LOL, SLOL- and IP-tuning using 6-311G(d) basis set on the reproduction of the experimental $\Delta E_{ST}$ (eV).

| Compound | LC-$\omega$PBE$^{LOL}$ | | LC-$\omega$PBE$^{IP}$ | | LC-$\omega$PBE$^{SLOL}$ | | Expt. |
|---|---|---|---|---|---|---|---|
| | $\Delta E_{VST}$ (Cyc.)[a] | $\Delta E_{AST}$ (Tol.)[b] | $\Delta E_{VST}$ (Cyc.)[a] | $\Delta E_{AST}$ (Tol.)[b] | $\Delta E_{VST}$ (CBP)[c] | $\Delta E_{VST}$ (Cyc.)[c] | $\Delta E_{ST}$[d] |
| PIC-TRZ | 0.33 | 0.15 | 0.22 | 0.15 | 0.11 | 0.1V0 | 0.17 |
| CC2TA | 0.35 | 0.25 | 0.37 | 0.25 | 0.10 | 0.09 | 0.30 |
| PXZ-TRZ | 0.02 | 0.08 | 0.02 | 0.08 | 0.01 | 0.01 | 0.03 |
| DPAC-TRZ | 0.02 | 0.22 | 0.02 | 0.22 | 0.01 | 0.01 | 0.16 |
| Cz-TRZ | 0.50 | 0.65 | 0.55 | 0.65 | 0.32 | 0.31 | 0.40 |
| Cz-TRZ2 | 0.02 | 0.27 | 0.06 | 0.27 | 0.01 | 0.01 | 0.31 |
| 3Cz-TRZ | 0.42 | 0.56 | 0.49 | 0.56 | 0.15 | 0.13 | 0.37 |
| BCz-TRZ | 0.39 | 0.57 | 0.46 | 0.57 | 0.23 | 0.21 | 0.39 |
| 2CzPN | 0.46 | 0.34 | 0.44 | 0.34 | 0.32 | 0.31 | 0.40 |
| 4CzPN | 0.17 | 0.15 | 0.13 | 0.15 | 0.11 | 0.11 | 0.25 |
| 4CzIPN | 0.15 | 0.12 | 0.13 | 0.12 | 0.12 | 0.12 | 0.12 |
| 4CzTPN | 0.17 | 0.08 | 0.15 | 0.08 | 0.13 | 0.13 | 0.01 |
| 4CzTPNMe | 0.15 | 0.01 | 0.13 | 0.01 | 0.10 | 0.09 | 0.01 |
| DPA-DPS | 0.63 | 0.49 | 0.64 | 0.49 | 0.56 | 0.54 | 0.47 |
| DTPA-DPS | 0.60 | 0.47 | 0.60 | 0.47 | 0.52 | 0.51 | 0.43 |
| DTC-DPS | 0.38 | 0.27 | 0.41 | 0.27 | 0.28 | 0.27 | 0.37 |
| DMOC-DPS | 0.56 | 0.34 | 0.62 | 0.34 | 0.26 | 0.25 | 0.31 |
| PXZ-DPS | 0.05 | | 0.06 | | 0.04 | 0.04 | 0.03 |
| DMAC-DPS | 0.02 | 0.13 | 0.02 | 0.13 | 0.01 | 0.01 | 0.14 |
| PPZ-DPS | 0.02 | 0.00 | 0.02 | 0.00 | 0.01 | 0.01 | 0.01 |
| DPA-AQ | 0.53 | 0.56 | 0.56 | 0.56 | 0.47 | 0.47 | 0.29 |
| DBPA-AQ | 0.48 | 0.48 | 0.50 | 0.48 | 0.43 | 0.42 | 0.27 |
| DTC-AQ | 0.32 | 0.31 | 0.37 | 0.31 | 0.25 | 0.25 | 0.17 |
| DMAC-AQ | 0.03 | 0.04 | 0.07 | 0.04 | 0.01 | 0.01 | 0.08 |
| DPA-Ph-AQ | 0.37 | 0.45 | 0.43 | 0.45 | 0.23 | 0.22 | 0.24 |
| DBPA-Ph-AQ | 0.32 | 0.53 | 0.42 | 0.53 | 0.18 | 0.17 | 0.22 |
| DTC-Ph-AQ | 0.39 | 0.25 | 0.43 | 0.25 | 0.12 | 0.11 | |
| DMAC-Ph-AQ | 0.40 | 0.32 | 0.44 | 0.32 | 0.001 | 0.001 | 0.07 |
| MAD | 0.12 | 0.10 | 0.13 | 0.10 | 0.10 | 0.10 | |
| RMSD | 0.09 | 0.08 | 0.10 | 0.10 | 0.07 | 0.07 | |
| Max Dev. | 0.33 | 0.27 | 0.37 | 0.31 | 0.30 | 0.30 | |

[a] Calculated in PCM cyclohexane solvation ($\varepsilon$ = 2.02); [b] Calculated in PCM toluene solvation ($\varepsilon$ = 2.37); [c] Using the static dielectric constant of CBP-doped thin film ($\varepsilon$ = 1.73) experimentally determined from the relaxed Lorentz model[2]. [d] Determined in 77 K toluene matrix except the Donor-AQ and Donor-Ph-AQ series.

References

1. Sun, H.; Zhong, C.; Bredas, J. L., Reliable Prediction with Tuned Range-Separated Functionals of the Singlet-Triplet Gap in Organic Emitters for Thermally Activated Delayed Fluorescence. *J. Chem. Theory Comput.* **2015,** *11* (8), 3851-3858.

2. Liu, Z. T.; Kwong, C. Y.; Cheung, C. H.; Djurišić, A. B.; Chan, Y.; Chui, P. C., The characterization of the optical functions of BCP and CBP thin films by spectroscopic ellipsometry. *Synth. Met.* **2005,** *150* (2), 159-163.